International Journal of Engineering

Journal Homepage: www.ije.ir

A Distributed Cooperative Secondary Control Scheme for Obtaining Power and Voltage References of Distributed Generations in Islanded DC Microgrids

M. Nabian Dehaghani[a], M. Biglarahmadi[a], S. Y. Mousazadeh Mousavi*[b], M. Abdolahi[c]

[a] *Department of Electrical Engineering, University of Kashan, Kashan, Iran*
[b] *Department of Electrical Engineering, Faculty of Technology and Engineering, University of Mazandaran, Babolsar, Iran*
[c] *Department of Electrical Engineering, Faculty of Electrical and Computer Engineering, Babol Noshirvani University of Technology, Babol, Iran*

P A P E R I N F O

Paper history:
Received 18 August 2023
Received in revised form 14 September 2023
Accepted 16 September 2023

Keywords:
DC Microgrids
Distributed Secondary Control
Droop Control
Power Sharing
Voltage Regulation

A B S T R A C T

Due to the widespread adoption of DC source-based distributed energy resources (DERs) and loads, alongside advancements in power electronics technology, DC microgrids (DC MGs) have recently gained significant attention. To effectively implement DC MGs, it is crucial to employ a suitable control strategy that maintains the bus voltage at the desired level and ensures appropriate power sharing among the integrated DERs. To address these objectives, a two-layer control scheme is proposed in this paper. In the primary layer, a customized droop control scheme is introduced, which applies lower voltage drop in comparison to the conventional droop strategies. Simultaneously, in the secondary layer, a modified voltage controller which is supplemented by a term to enhance power sharing in a distributed manner is employed,. The proposed control strategies are characterized by their simplicity and low communication infrastructure requirements. To assess the efficacy of the proposed control architecture, several case studies, including plug and play integration, load variations, and communication challenges, including link disconnection and noise effects, are conducted. Additionally, the performance of the proposed strategies is benchmarked against an architecture featuring conventional primary droop control and cooperative distributed secondary control approaches. The simulation studies conducted in MATLAB/SIMULINK software demonstrate that the proposed control methods outperform the alternative approaches, confirming their effectiveness in maintaining voltage regulation and power sharing objectives.

doi: *10.5829/ije.2024.37.02b.10*

Graphical Abstract

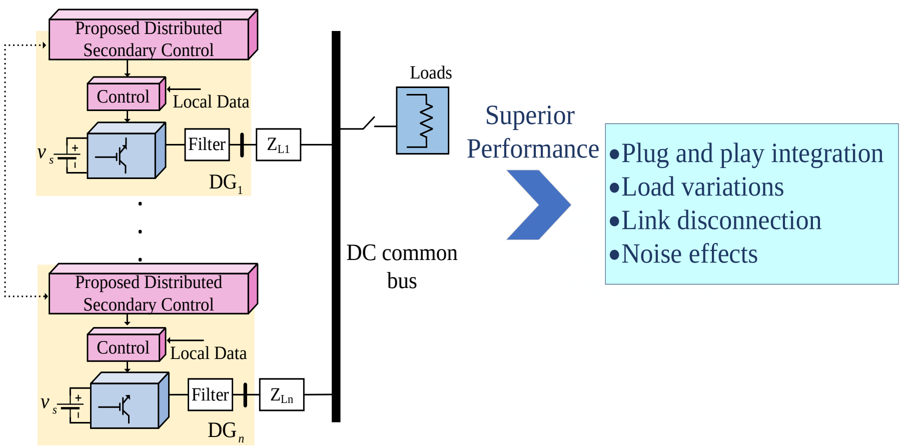

*Corresponding Author Email: s.y.mousazadeh@umz.ac.ir (S. Y. Mousazadeh Mousavi)

Please cite this article as: Nabian Dehaghani M, Biglarahmadi M, Mousazadeh Mousavi SY, Abdolahi M. A Distributed Cooperative Secondary Control Scheme for Obtaining Power and Voltage References of Distributed Generations in Islanded DC Microgrids, International Journal of Engineering, Transactions B: Applications. 2024;37(02):341-51.

1. INTRODUCTION

In recent years, there has been a growing interest in the microgrid (MG) concept as a means of reliability enhancement, improvement in power quality, and integration of renewable energy resources (RESs) (1, 2). The control of MGs, all types of AC, DC, and AC/DC MGs, in both their operational inslanded and grid-connected modes is the main interest of many researchers (3). The use of DC MGs has particularly gained attention due to the evolution in power electronics technology, more compatibility with other equipment, and greater flexibility in integrating of RERs and energy storage systems into the grid (4). In DC MGs, distributed generation (DG) units are mainly connected to MGs through power electronic interfaces, and the control of parallel DC-DC converters becomes essential (5). The droop control method is the most prevalent control approach employed for DC MGs, which enables cooperative control of power electronic interfaces without the communication link requirements (6). The droop control approach is based on an inner control loop, as a virtual resistance control, which facilitates simultaneous current and power-sharing while offering a plug-and-play feature (7, 8).

The conventional droop method is based on analyzing the output currents and voltages of power electronic interfaces. However, its implementation faces certain challenges. To gain appropriate operation in terms of power sharing, the droop coefficients should be significantly larger than the line resistances. Although the larger values lead to more accurate power sharing, they also create higher voltage drops. Conversely, the smaller values, the better voltage adjustment and the poorer power sharing. As a result, striking a balance between permissible voltage drop and accurate power sharing becomes essential (9). A further issue arises from the fact that line resistances of DG units are mostly different, which adversely impacts both voltage adjustment and power sharing (10).

Various modified droop control methods have been introduced in the existing literature to achieve precise current sharing and voltage regulation in paralleled converters of DC MGs (11-19). It is worth mentioning that modified droop methods are also popular in AC MGs as well (20). An observer-based droop control combined with current feed-forward control was proposed by Li et al. (11) to address the trade-off between the current sharing and the dynamic stability in a DC MG. Both feedback and feed-forward currents were provided by the observer without any additional measurement requirement, resulting in cost reduction. The system's stability, dynamics, and plug-and-play capability were improved as well. Sukhadiaa and Saurabh (12) proposed a droop index for the parallel operation DC converters in low-voltage DC (LVDC) MGs. Their adaptive droop control scheme was based on a function of the normalized current sharing differences of DG units and the power losses, effectively minimizing the circulating current and the current sharing differences. Consequently, the trade-off between voltage regulation and current sharing difference was eliminated. An adaptive droop control algorithm incorporating estimated line resistances was introduced by Ghanbari and Bhattacharya (14), where droop coefficients were set according to these resistances, reducing the line resistance impact on the accurate power sharing. Moreover, a hybrid droop based coordination scheme is recommended by Saeidinia et al. (15) for a class of DC MG that can simultaneously optimize the total generation cost and total transmission power loss. Additionally, a distributed secondary controller was presented to restrain the circulating currents. In the context of interlinking converters connecting AC grids with LVDC subgrids, a selective power droop control approach was proposed by Wang et al. (16)to overcome challenges related to high capacitive coupling impedance and low converter capacity in LVDC grids. The conventional droop strategy was enhanced by Shehata et al. (17) with an online adaptation algorithm that updated the droop coefficients according to the voltage deviation and the current difference. Similarly, a modified droop controller was adopted by Bharath et al. (18), where the droop coefficient was treated as an output voltage-based function, leading to superior voltage adjustment. An adaptive droop control strategy for DC MGs, capable of adapting to the load changes, was established by Shaheed et al. (19). The control approach proposed by Khanabdal et al. (20) exhibited acceptable current sharing performance without requiring any optimization.

In contrast, the previous references did not fully consider the nonlinearity of the system, especially when passive loads, such as resistive ones, are presented in the external characteristics of converters. To address this limitation, the $V_{dc}^2 - P_{dc}$ droop strategy was implemented by Xia et al. (21) for sharing of power and regulating voltage among multiple energy storage units. This decentralized method enhanced system performance and reliability compared to other strategies due to the linear relationship between V_{dc}^2 and P_{dc}, while the relationship between V_{dc} and i_{dc} is nonlinear. Notably, this method is applied here to the primary layer of DG units, which had not been previously considered for the control of DG units further highlighting its outperformance.

The aforementioned droop control methods have not achieved simultaneous precise power sharing and voltage adjustment. Even though the proposed $V_{dc}^2 - P_{dc}$ controller outperforms other primary droop controllers, it still requires a correction term as a secondary controller. Another issue with droop control methods and their derivatives is the lack of a coordinated operation. Therefore, a secondary controller is necessary to address these challenges (22). To achieve this, the centralized, decentralized, or distributed secondary strategies are needed. There are a variety of available approaches, with traditional methods based on centralized control (23) and recent literature focusing on distributed control techniques (24-36). Distributed methods are preferred due to their high reliability and the sparse communication graph requirements.

For instance, a conventional droop-based primary control, along with a feedback-based distributed secondary control, was proposed by Guo et al. (28), for power sharing and voltage restoration in islanded DC MGs. The control apprcoach proposed by Guo et al. (28) required only bus voltages measurment. Aimed to suppress the effects of noise disturbances, a distributed cooperative strategy was introduced by Nabian et al. (29); this secondary controller proposed by Nabian et al. (29) involved two correction terms, one for the voltage and another for the current, and utilized the average voltage of neighboring units. Similar distributed secondary voltage controllers were presented by Biglarahmadi (30) and Nabian et al. (31) for the coordination of DG units in the DC subgrid of hybrid AC/DC MGs, operating under the load changes and the communication link interruption. Guo et al. (33) proposed a distributed attack resilient secondary control method with consensus-based current and average consensus-based voltage regulators, but this method comes with a high computational burden. A two-layer multi-agent based distributed control scheme, comprising physical and cyber voltage restoration layers, is proposed by Fan et al. (34). The control strategy proposed by Fan et al. (34) required only feedback of DC bus voltage and overall system information was not required, however it lacks in-depth discussions on precise power sharing. Another distributed consensus based secondary scheme was suggested Xing et al. (35) for DC MGs in the presence of different loads. This approach utilized a global weighted average voltage in its distributed secondary controller, however, it also involved with a high computational burden. Lastly, Keshavarz et al. (36) considered a new parameter called 'virtual voltage drop' for the secondary control layer, which combined the droop gain and line resistance.

The literature offers various distributed secondary control methods to address challenges in achieving the coordinated operation of DG units and the precise power sharing of them, but each approach comes with its own set of advantages and limitations. The $V_{dc}^2 - P_{dc}$ droop control method addresses the voltage adjustment and the power-sharing (21). Although modifications have been made to the primary droop controllers, achieving accurate power sharing, presice voltage adjustment, and noise disturbance elimination simultaneously remains some challanges. Therefore, the incorporation of a distributed secondary controller becomes essential to accomplish these objectives more effectively. Furthermore, the proposed approach demonstrates enhanced voltage regulation, improved current sharing, and noise nullification compared to data reported in literature (28).

A power sharing improvement term has also been introduced in this study, enabling performance to be improved in scenarios involving communication link interruptions. In summary, the main contributions of this paper are the following:

- The modified distributed secondary control (MDSC) method is designed to effectively cancel noises by approximating the global average voltage through the estimation of local and neighbouring voltages, achieved by nullifying the noise. In comparison with literature (28, 33), this method demonstrates superior noise mitigation capabilities.
- The proposed MDSC method exhibits efficient performance under the load changes, the plug-and-play scenarios, and the communication link malfunctions. This technique demonstrates precise tracking of the reference voltage and achieves nominal voltage with high convergence speed and without overshoot or undershoot, with accurate power sharing as well, as compared to the method described by Keshavarz et al. (36).
- Instead of the conventional droop method, the $V_{dc}^2 - P_{dc}$ approach is employed at the primary control level of DG units. Although this method was previously implemented in voltage adjustment for energy storage units of hybrid MGs (as reported by Xia et al. (21)), it is now applied to the controllers of DG units for the first time. Furthermore, its interaction with the proposed MDSC method is taken into consideration.

The rest of this paper is organized as follows. In section 2, the customized droop method is explained. The proposed secondary control method is discussed in section 3 .The simulation results are presented in section 4 and finally, section 5 concludes this paper.

2. $V_{dc}^2 - P_{dc}$ DROOP METHOD

The general overview of a DC MG with its controllers is demonstrated in Figure 1. As it is shown, each DG unit can be presented with a DC/DC converter connected to photovoltaic (PV) or other generation units. DGs are connected to respective buses with line impedances. The DC MG can be connected to the main grid, even though the understudied DC MG works in islanded mode.

This section presents a $V_{dc}^2 - P_{dc}$ approach for the primary control level. As observed, the conventional

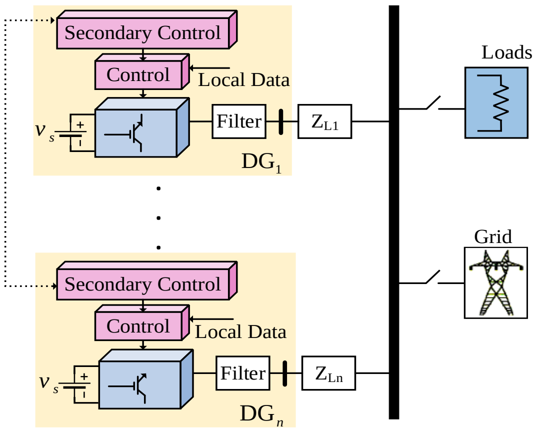

Figure 1. General overview of the DC MG

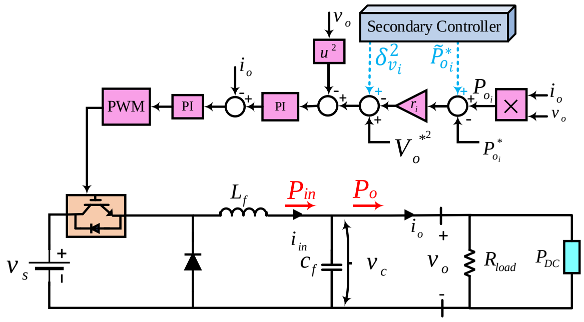

Figure 2. The typical diagram of a DC DG with primary controller and its simplified circuit diagram with connected loads

droop method, which is based on the relationship between voltage and current, needs a precise tradeoff among power sharing accuracy and voltage regulation (28); hence, the droop control approach based on the relationship between the square of voltage and output power designed by Xia et al. (21) and implemented for energy storage units is considered for the primary control level of DG units in this paper. The typical diagram of a DG which is connected by a DC/DC converter to the DC common bus is shown in Figure 2. According to this figure, the relationship between the output current and voltage ($v_o - i_o$) can be expressed as folows (21):

$$\begin{cases} c_f \dfrac{dv_c}{dt} = i_{in} - i_o, \\ v_c = v_o, \\ i_o = v_o R_{load} + \dfrac{P_{DC}}{v_o} \end{cases} \tag{1}$$

In the above equation, c_f, R_{load}, P_{DC}, i_{in}, and v_c represent filter capacitance, load resistance, DC power, input current, and capacitance voltage, respectively. As it is obvious, the relationship of $v_o - i_o$ is nonlinear which means if the traditional droop method is employed, the efficiency of regulations will be reduced.

Despite all that, the forthcoming equations can be written if the balance of power in Figure 2 is taken into account (21).

$$\left. \begin{aligned} c_f \frac{dv_o^2}{dt} &= P_{in} - P_o \\ P_o &= \frac{v_o^2}{R_{load}} + P_{DC} \end{aligned} \right\} \Rightarrow c_f \frac{dv_o^2}{dt} = P_{in} - \frac{v_o^2}{R_{load}} - P_{DC} \tag{2}$$

where P_{in} and P_o are the input and the output powers. It is obvious that there is a linear relationship between v_o^2 and P_o. As a result, a droop method based on $P - v_o^2$ can be derived in order to improve the accuracy of the control system. This method is composed of two inner and outer loops, the former controlling the v_o^2 and the later considering the power sharing.

If the switch and filter losses are neglected, the average model of the converter can be written as follows (21):

$$\begin{cases} \dfrac{1}{2} c_f \dfrac{dv_o^2}{dt} = v_s . i_{in} - P_o \\ L_f \dfrac{di_{in}}{dt} = v_s - v_o \end{cases} \tag{3}$$

where L_f and v_s represent the filter inductance and the voltage of primary resource, respectively. With regard to this equation, the inner loop can be illustrated as Figure 2. A proportional-integral (PI) controller for the voltage controller is employed in order to eliminate static errors, while a proportional controller is utilized for the current controller in order to intensify damping. Next, the customized $P_o - v_o^2$ o droop, as outer loop, can be analyzed and formulized as follows (21).

$$v_{o_i}^{ref^2} = V_o^{*2} - r_i \left(P_{o_i} - P_{o_i}^* \right) \tag{4}$$

where $v_{o_i}^{ref^2}$, V_o^{*2}, r_i, P_{o_i}, and $P_{o_i}^*$ represent reference output voltage value, rated output voltage value, droop coefficient, measured output power, and rated output power, respectively; subscript of i denotes the i^{th} converter. Besides, the following equation should be satisfied if it is required to ensure appropriate current sharing while load changes (21).

$$\frac{r_i}{r_j} = \frac{P_{o_j}^*}{P_{o_i}^*} \tag{5}$$

3. DISTRIBUTED SECONDARY CONTROL FOR VOLTAGE RESTORATION

In this part, the proposed MDSC method, which is depicted in Figure 3(a), is explained. As a result, the following term is regarded as the secondary correction voltage, and is written in the following manner:

$$\delta_{v_i} = \left(k_p + \frac{k_i}{s}\right) e_i \tag{6}$$

where k_p and k_i represent the PI parameters and e_i is total error, which can be expressed as follows:

$$e_i = g_i\ \alpha_i\ e^v + \beta_i e^{\delta_{v_i}} \tag{7}$$

In the above equation, α_i, β_i, and g_i are control error and restoration error gains and pinning gain ($g_i \neq 0$ for the reference agent), respectively; $e^{\delta_{v_i}}$ denotes the control error and e^v represents the error of restoring voltage. These recent terms are defined as follows:

$$\begin{cases} e^v = v_o^* - v_o \\ e^{\delta_{v_i}} = \sum_{j \in N} a_{ij}\left(\delta_{v_j} - \delta_{v_i}\right) \end{cases} \tag{8}$$

where a_{ij} is the edge weight among i th and j th DG. As one of the aims of this controller is voltage restoration, then:

$$\begin{cases} \lim_{t \to \infty} e^v(t) = 0 \\ \lim_{t \to \infty} e^{\delta_{v_i}}(t) = 0 \end{cases} \tag{9}$$

The performance of the proposed voltage controller can be influenced if disturbances exist; hence, a term should be considered for nullification of noises. This term is defined as follows:

$$u_i = v_i - \delta_{v_i} \tag{10}$$

A white noise source, which is illustrated by d_i in Figure 3 is exerted. To do this and ensure accurate disturbance tracking, u_i is sent to an integrator. Afterward, the average value of this term can be rewritten as follows:

$$\dot{\bar{u}}_i(t) = u_i(t) + \int_0^t \sum_{j \in N} ai_j\left(\bar{u}_j(\tau) - \bar{u}_i(\tau)\right) d\tau \tag{11}$$

The following protocol is attained by differentiation of Equation 11.

$$\dot{\bar{u}}_i(t) = u_i(t) + \sum_{j \in N} ai_j\left(\bar{u}_j - \bar{u}_i\right) \tag{12}$$

Eventually, $\tilde{d}_i$, as the noise deactivation term, is defined as follows:

$$\tilde{d}_i = \frac{k_i}{s}\bar{u}_i \tag{13}$$

In the end, the new forthcoming term is assumed as the reference voltage value for the primary controller.

$$\delta_{v_i}^{'2} = \left(k_p + \frac{k_i}{s}\right) e_i + d_i - \tilde{d}_i \tag{14}$$

The other aim of the secondary controller is to make the output power track its reference value meticulously. As a result, a PI controller is adopted because of its capability to omit the steady state error as follows:

$$\tilde{P}_{o_i}^* = \left(k_{P_p} + \frac{k_{P_i}}{s}\right)\left(P_{o_i}^* - P_{o_i}\right) \tag{15}$$

where k_{P_p} and k_{P_i} represent the PI coefficients and $\tilde{P}_{o_i}^*$ is produced reference power, which is named as virtual power control reference. It will be utilized as the reference value of the primary controller. For achieving better and more accurate current sharing, the following term is also added by considering the output powers and the droop coefficients of other DGs.

$$\delta_p = \sum_{j \in N} a_{ij}\left(r_j P_{o_j} - r_i P_{o_i}\right) \tag{16}$$

where δ_p denotes the power correction term. The final virtual power reference ($\tilde{P}_{o_i}^*$) which is added to $P_{o_i}^*$ in the primary controller can be rewritten as follows:

$$\tilde{P}_{o_i}^* = \left(k_{P_p} + \frac{k_{P_i}}{s}\right)\left(P_{o_i}^* - P_{o_i}\right) + \delta_p \tag{17}$$

The overall structure of this controller is illustrated in Figure 3(b).

4. SIMULATION RESULTS

For validating the proposed CDM and MDSC methods in DC MGs, a typical DC MG which is depicted in Figure 4 is simulated in MATLAB/SIMULINK software. This MG is composed of 4 DG units and 800W loads; the

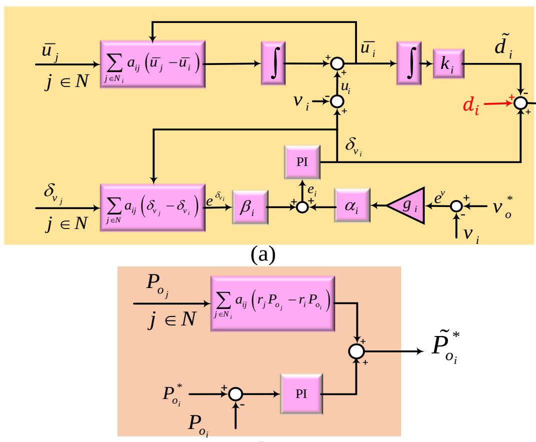

(a)

(b)

Figure 3. Control block diagram of the MDSC method (a) the voltage correction term (b) the power correction term $\delta_{v_i}^{'2}$ is added to the primary controller (the blue one in Figure 2)

nominal produced power of DGs is considered as 200W. The parameters of DGs, lines, and other data can be found in Table 1. To confirm the efficiency of the proposed method, different case studies are considered and results are also compared with other methods, including the conventional primary droop method and proposed distributed secondary control methods (28, 35) for better evaluation. The case studies are as follows:

- Case I: The DC MG works with either conventional droop or $V_{dc}^2 - P_{dc}$ droop method;
- Case II: At *t = 1.5s*, the voltage restoration part of the MDSC method and the methods of Guo et al. (28) and Keshavarz et al. (36) are activated for each respective simulation;
- Case III: The power correction term of the MDSC method is subsequently added at *t = 2.5s*, so its efficiency is more sensible;
- Case IV: There is a load increase at *t = 3.5s* (its power equals 200W);
- Case V: DG_4 is plugged out at *t = 4.5s*, and reconnected at *t = 6s*;
- Case VI: At *t = 7.5s*, the communication link between DG_2 and DG_3 is missed and it is restored at *t = 9s*;
- Case VII: Finally, a white noise is considered at *t = 10.5s*.

It is worth mentioning that a graph should be assumed to demonstrate the communication links among DGs. The following equation shows the corresponding adjacency matrix. According to this matrix, there is a unilateral connection which reduces the volume of data.

$$A = \begin{bmatrix} 0 & 0 & 0 & 1 \\ 1 & 0 & 0 & 0 \\ 0 & 1 & 0 & 0 \\ 0 & 0 & 1 & 0 \end{bmatrix} \tag{18}$$

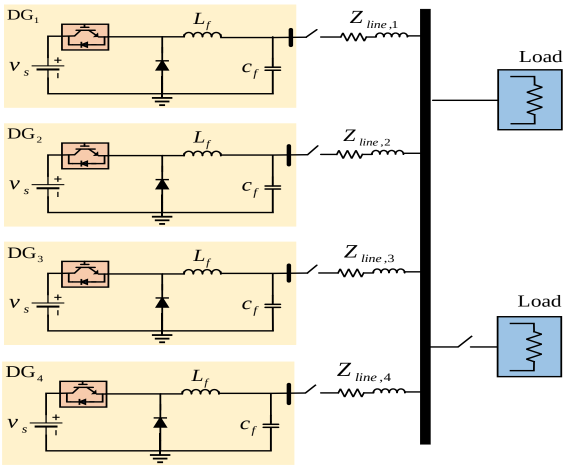

Figure 4. Structure of the studied DC MG

TABLE 1. Parameters of DC MG

Symbol	Quantity	Value
V_o	Nominal DC voltage	48 V
k_{p_v}	Proportional term of voltage controller	1
k_{i_v}	Integral term of voltage controller	250
k_{p_i}	Proportional term of current controller	5
k_{i_i}	Integral term of voltage controller	100
$r_{1\&2}$	DG1&DG2 Droop coefficients	$5\ V^2/W$
$r_{3\&4}$	DG3&DG4 Droop coefficients	$3\ V^2/W$
	Secondary parameters	
α_i	control error gain	1
β_i	restoration error gain	1
k_i	Integral term of secondary voltage controller	1
$k_{P\&I}$	Proportional term of secondary power controller	1 & 40

The obtained results are presented in Figures 5-10 as follows.

The results of Cases I-IV are illustrated in Figures 5(a)-(f) and 6(a)-(f). As it is obvious, when the primary controllers are merely activated, the proposed $V_{dc}^2 - P_{dc}$ droop method shows superior performance (Figures 5 and 6 (b)) and the voltage drop is lower in comparison with results obtained by the conventional droop controller (Figure 5 and 6(a)). As long as the secondary method of (28, 36) and the proposed MDSC method are employed in respective simulations, although both strategies restore the voltage to its nominal value, no overshoot can be observed for implementing the MDSC method and it also converges faster. In addition, when the correction power term of the MDSC method is implemented (*t = 2.5s*), power and current sharing are improved subsequently (see Figures 5 and 6(d) & (f)). Moreover, while load changes, it is manifest that the voltage drop of proposed methods is ignorable, while there is an observable drop for voltage obtained by the method of Keshavarz et al. (36). For a more precise comparison, Table 2 provides the voltage error percentages for each case. The time required to approach nominal values is compared in Table 3. It should be mentioned that both simulations are performed in similar situations and both by 8 GB RAM, Core i7-2670QM CPU system.

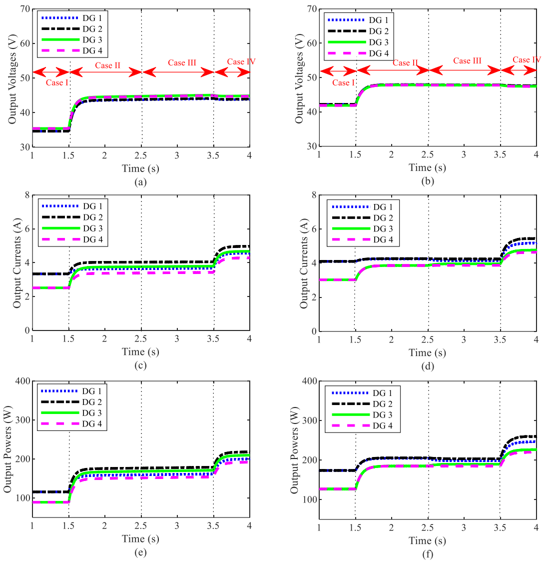

Figure 5. Results obtained in Cases I-IV. (a) Output voltage obtained by method of (28); (b) Output voltage obtained by proposed $V_{dc}^2 - P_{dc}$ droop and MDSC methods; (c) Output current obtained by method of (28); (d) Output current obtained by proposed $V_{dc}^2 - P_{dc}$ droop and MDSC methods; (e) Output power obtained by method of (28); (f) Output power obtained by proposed $V_{dc}^2 - P_{dc}$ droop and MDSC methods

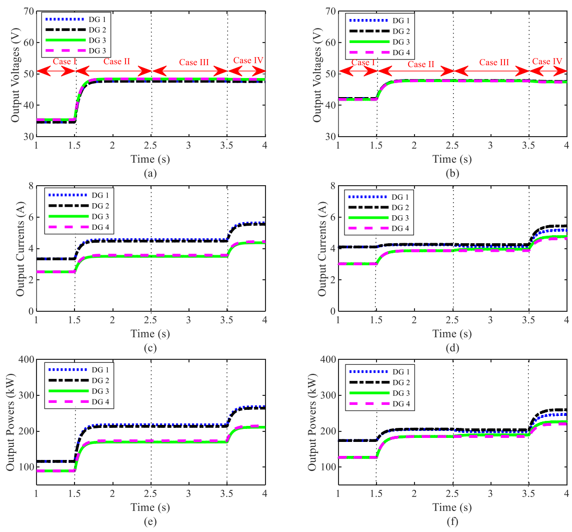

Figure 6. Results obtained in Cases I-IV. (a) Output voltage obtained by method of (36); (b) Output voltage obtained by proposed $V_{dc}^2 - P_{dc}$ droop and MDSC methods; (c) Output current obtained by method of (36); (d) Output current obtained by proposed $V_{dc}^2 - P_{dc}$ droop and MDSC methods; (e) Output power obtained by method of (36); (f) Output power obtained by proposed $V_{dc}^2 - P_{dc}$ droop and MDSC methods

TABLE 2. Comparison of errors in different cases

Index	$e_{V_i}(\%) = \frac{V_{ref} - V_i}{V_{ref}} \times 100$							
	Case	**1**	**2**	**3**	**4**	**5**	**6**	**7**
Conventional droop and method of (28)	DG_1	27.91	7.1	-	6.69	25.68	6.9	6.04
	DG_2	27.91	7.05	-	6.65	23.23	6.76	5.83
	DG_3	26.25	8.93	-	8.52	19.37	4.79	3.75
	DG_4	26.25	8.93	-	8.56	-	5	3.95
Conventional droop and method of (36)	DG_1	27.91	0.416	-	1.341	2.083	1.666	-6.73
	DG_2	27.91	0.416	-	1.341	2.083	1.145	-6.73
	DG_3	26.25	0.833	-	1.537	0.83	2.083	-7.41
	DG_4	26.25	0.833	-	1.537	-	1.145	-7.41
$V_{dc}^2 - P_{dc}$ droop and MDSC methods	DG_1	10.83	0.145	-	0.719	1.666	0.729	0.729
	DG_2	10.83	0.145	-	0.719	1.666	0.583	0.729
	DG_3	12.72	0.354	-	0.921	1.395	1.145	0.937
	DG_4	12.72	0.354	-	0.921	-	0.583	0.937
Index	$e_{P_i}(\%) = \left(\frac{P_i}{\sum P_i} - \frac{P_{rated}}{\sum P_{rated}}\right) \times 100$							
	Case	**1**	**2**	**3**	**4**	**5**	**6**	**7**
Conventional droop and method of (28)	DG_1	5.048	-0.65	-	-0.31	-18.04	-1.02	-1.28
	DG_2	5.048	1.8	-	0.8	9.78	1.43	0.65
	DG_3	-5.048	0.88	-	0.93	33.26	0.73	1.22
	DG_4	-5.048	-2.03	-	-1.42	-	-1.14	-0.59
Conventional droop and method of (36)	DG_1	5.048	2.272	-	3.010	8.96	3.125	2.574
	DG_2	5.048	2.272	-	3.010	8.96	3.125	6.412
	DG_3	-5.048	-2.272	-	-3.010	10.507	-3.125	-3.5
	DG_4	-5.048	-2.272	-	-3.010	-	-3.125	-3.5
$V_{dc}^2 - P_{dc}$ droop and MDSC methods	DG_1	3.903	1.282	0.410	0.941	3.295	-0.376	0.492
	DG_2	3.903	1.282	1.089	1.696	3.295	-0.376	0.492
	DG_3	-3.903	-1.282	-0.641	-1.15	3.077	-1.188	-1.188
	DG_4	-3.903	-1.282	-1.282	-1.987	-	-1.188	-1.542

TABLE 3. Comparison of time to reach nominal values (s)

	Ref.	**[28]**	**[35]**	**This paper**
After activation of Sec. Controller	V	0.23	0.15	0.15
	I	0.2	0.1	0.1
	P	0.22	0.2	0.2
After applying noise	V	1.45	0.9	0.01
	I	1.425	1	0.01
	P	1.985	1	0.02

Results for the efficiency evaluation of proposed methods in plug-and-play condition (Case V) are depicted in Figures 7 (a)-(f) and 8(a)-(f). It can be deemed that when DG_4 is disconnected, the method of Guo et al. (28) is unable to restore voltages and it takes some seconds to restore the voltage by using the method of Keshavarz et al. (36) (Figures 7 and 8(a)); however, the proposed methods properly remained stable (Figures 7 and 8(b)). Besides, when DG_4 is reconnected, it is completely clear that there is a significant overshoot for results obtained by the method of Keshavarz et al. (36), and even after 1s, it is not able to restore the stable condition in the studied MG (Figure 8(c)); by the method of Guo et al. (28), it takes more than *5s* to become stable (Figures 7(c)), though the results achieved by proposed strategies appropriately restore the voltage and other parameters without any overshoot (Figures 7 and 8(d)). The respective errors are given in Table 2. Eventually, Figures 9 (a)-(f) and 10 (a)-(f) show the results for Cases VI and VII. It can observed that when the communication link between DG_2 and DG_3 is lost, there is a conspicuous drop in the voltage and power of DG_2 by methods of Guo et al. (28) and Keshavarz et al. (36). Since white noise is inserted, despite methods of (28, 36), the proposed strategies work efficiently in the existence of noise and remain stable. To compare the results properly, the respective error percentages are presented in Table 2. It is obvious from the table that when the presented control methods are considered, the

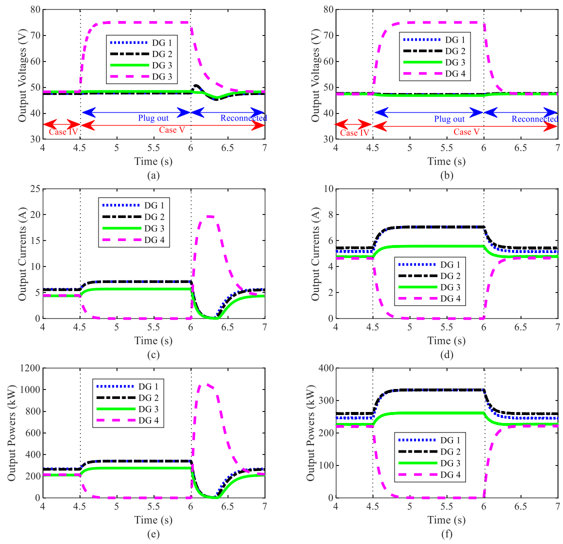

Figure 8. Results obtained in Cases V. (a) Output voltage obtained by method of (36); (b) Output voltage obtained by proposed $V_{dc}^2 - P_{dc}$ droop and MDSC methods; (c) Output current obtained by method of (36); (d) Output current obtained by proposed $V_{dc}^2 - P_{dc}$ droop and MDSC methods; (e) Output power obtained by method of (36); (f) Output power obtained by proposed $V_{dc}^2 - P_{dc}$ droop and MDSC methods

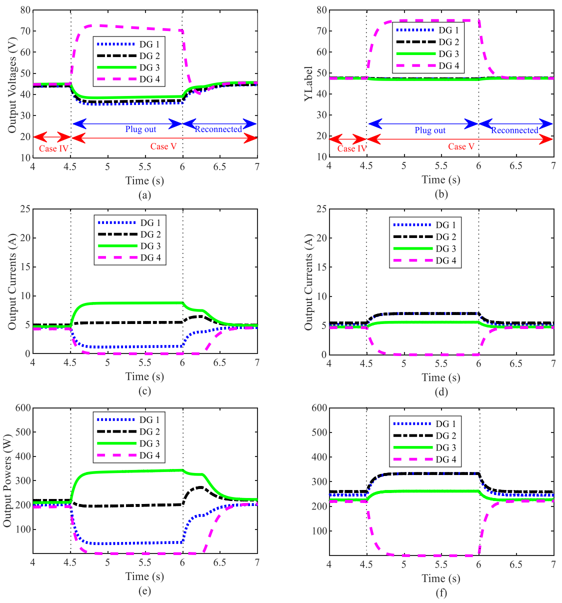

Figure 7. Results obtained in Cases V. (a) Output voltage obtained by method of (28); (b) Output voltage obtained by proposed $V_{dc}^2 - P_{dc}$ droop and MDSC methods; (c) Output current obtained by method of (28); (d) Output current obtained by proposed $V_{dc}^2 - P_{dc}$ droop and MDSC methods; (e) Output power obtained by method of (28); (f) Output power obtained by proposed $V_{dc}^2 - P_{dc}$ droop and MDSC methods

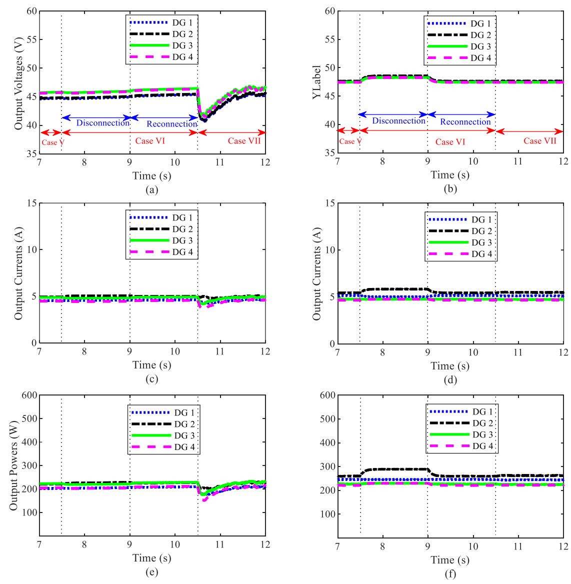

Figure 9. Results obtained in Cases VI-VII. (a) Output voltage obtained by method of (28); (b) Output voltage obtained by proposed $V_{dc}^2 - P_{dc}$ droop and MDSC methods; (c) Output current obtained by method of (28); (d) Output current obtained by proposed $V_{dc}^2 - P_{dc}$ droop and MDSC methods; (e) Output power obtained by method of (28); (f) Output power obtained by proposed $V_{dc}^2 - P_{dc}$ droop and MDSC methods

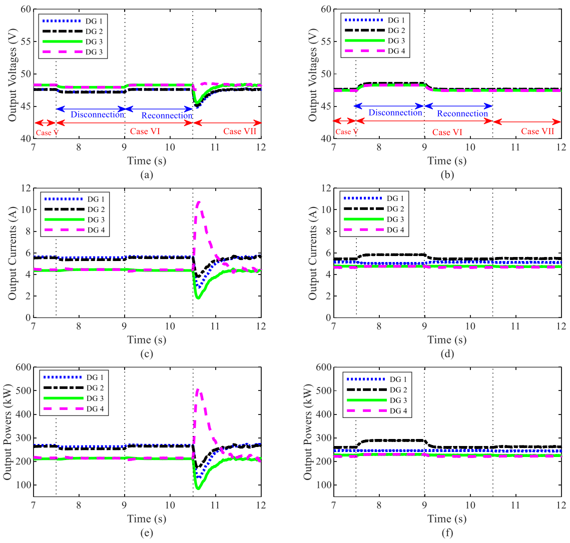

Figure 10. Results obtained in Cases VI-VII. (a) Output voltage obtained by method of (36); (b) Output voltage obtained by proposed $V_{dc}^2 - P_{dc}$ droop and MDSC methods; (c) Output current obtained by method of (36); (d) Output current obtained by proposed $V_{dc}^2 - P_{dc}$ droop and MDSC methods; (e) Output power obtained by method of (36); (f) Output power obtained by proposed $V_{dc}^2 - P_{dc}$ droop and MDSC methods

errors are in the acceptable range, while by implementing other methods (28, 36), there are considerable errors. The conventional droop-based primary controller along with the method of Guo et al. (28) is unable to share power and regulate voltage, especially when a disturbance such as plugging out of DG occurs.

Additionally, when the secondary proposed controller is activated, the time needed to reach the desired valuses are to some extent similar based on Table 3. However, if the noise is applied, the method of this paper can more effectively perform and has comparable better results compared to the methods of (28, 36). As observed, the strategy of Guo et al. (28) requires more than *1.5 s* to overcome this challenge; that of Keshavarz et al. (36) is almost *1 s*, while the proposed scheme approaches desirable values less than *0.05 s*.

5. CONCLUSION

This paper introduces a two-layer control structure aimed at effectively managing voltage control, accurately sharing current, and precisely performing across various operational scenarios as well as noise existence. To achieve this, a customized droop strategy was implemented in the first layer, resulting in reduced voltage drop and improved power sharing in comparison with conventional droop strategies. Furthermore, a distributed secondary controller incorporating voltage and power correction terms was integrated into the primary level to regulate the voltage at its nominal value and enhance precision in power allocation. Comparative analysis was conducted, revealing that the proposed $V_{dc}^2 - P_{dc}$ droop and MDSC methods outperformed the examined case studies in terms of less overshoot and faster convergence. Additionally, the effectiveness of the proposed methods was demonstrated when subjected to white noise injection.

6. REFERENCES

1. Sagar G, Debela T. Implementation of optimal load balancing strategy for hybrid energy management system in dc/ac microgrid with pv and battery storage. International Journal of Engineering, Transactions A: Basics. 2019;32(10):1437-45. 10.5829/IJE.2019.32.10A.13
2. Khanalizadeh Eini M, Mirhosseini Moghadam M, Tavakoli A, Alizadeh B. Stability Analysis of AC/DC Microgrids in Island Mode. International Journal of Engineering, Transactions A: Basics. 2021;34(7):1750-65. 10.5829/IJE.2021.34.07A.20
3. Norozpour Niazi A, Vasegh N, Motie Birjandi A. An Improved Hierarchical Control Structure for Robust Microgrid Operation and Seamless Mode Transfer under Linear and Nonlinear Loads conditions. International Journal of Engineering, Transactions C: Aspects. 2021;34(9):2167-79. 10.5829/IJE.2021.34.09C.14
4. Chen Y-K, Wu Y-C, Song C-C, Chen Y-S. Design and implementation of energy management system with fuzzy control for DC microgrid systems. IEEE Transactions on power electronics. 2012;28(4):1563-70. 10.1109/TPEL.2012.2210446
5. Abdolahi M, Adabi J, Mousavi SYM. An Adaptive Extended Kalman Filter with Passivity-Based Control for DC-DC Converter in DC Microgrids Supplying Constant Power Loads. IEEE Transactions on Industrial Electronics. 2023. 10.1109/TIE.2023.3283686
6. Nejabatkhah F, Li YW. Overview of power management strategies of hybrid AC/DC microgrid. IEEE Transactions on power electronics. 2014;30(12):7072-89. 10.1109/TPEL.2014.2384999
7. Dragičević T, Lu X, Vasquez JC, Guerrero JM. DC microgrids—Part II: A review of power architectures, applications, and standardization issues. IEEE transactions on power electronics. 2015;31(5):3528-49. 10.1109/TPEL.2015.2464277
8. Khorsandi A, Ashourloo M, Mokhtari H. A decentralized control method for a low-voltage DC microgrid. IEEE Transactions on Energy Conversion. 2014;29(4):793-801. 10.1109/TEC.2014.2329236
9. Elrayyah A, Cingoz F, Sozer Y. Smart loads management using droop-based control in integrated microgrid systems. IEEE Journal of Emerging and Selected Topics in Power Electronics. 2017;5(3):1142-53. 10.1109/JESTPE.2017.2666786
10. Kumar R, Pathak MK. Distributed droop control of dc microgrid for improved voltage regulation and current sharing. IET Renewable Power Generation. 2020;14(13):2499-506. 10.1049/iet-rpg.2019.0983
11. Li X, Guo L, Zhang S, Wang C, Li YW, Chen A, et al. Observer-based DC voltage droop and current feed-forward control of a DC microgrid. IEEE Transactions on Smart Grid. 2017;9(5):5207-16. 10.1109/TSG.2017.2684178

12. Sukhadiaa R, Pandya S, editors. Modified Droop Control Strategy for Load Sharing and Circulating Current Minimization in Low-Voltage Standalone DC Microgrid. Advances in Control Systems and its Infrastructure: Proceedings of ICPCCI 2019; 2020: Springer. 10.1007/978-981-15-0226-2_5
13. Zhao W, Duan M, Dong Y, Wang G, Pan Y, Tang M, et al., editors. An Adaptive Dynamic Droop Control Strategy for Load Sharing and Voltage Regulation in Low-Voltage DC Microgrid. 2021 IEEE Sustainable Power and Energy Conference (iSPEC); 2021: IEEE. 10.1109/iSPEC53008.2021.9735666
14. Ghanbari N, Bhattacharya S. Disturbance rejection analysis of a droop-controlled dc microgrid through a novel mathematical modeling. IEEE Journal of Emerging and Selected Topics in Power Electronics. 2021;10(2):1507-18. 10.1109/JESTPE.2021.3088777
15. Saeidinia Y, Arabshahi M, Mousazadeh Mousavi SY, Biglari M. Autonomous control of DC microgrid based on a hybrid droop control scheme for total generation cost and transmission power loss reduction. Electrical Engineering. 2023;105(1):267-83. 10.1007/s00202-022-01662-w
16. Wang L, Wong M-C, Zhou X, He Z, Xu Q, Zhou L. A selective power droop control for hybrid interlinking converter in AC/LVDC microgrid. IEEE Transactions on Industrial Electronics. 2020;68(10):9046-57. 10.1109/TIE.2020.3020017
17. Shehata E, Thomas J, Mostafa R, Ghalib M, editors. An improved droop control for a low voltage DC microgrid operation. 2018 Twentieth International Middle East Power Systems Conference (MEPCON); 2018: IEEE. 10.1109/MEPCON.2018.8635258
18. Bharath K, Dayal A, Kanakasabapathy P, editors. A simulation study on modified droop control for improved voltage regulation in DC microgrid. 2017 International Conference on Intelligent Computing, Instrumentation and Control Technologies (ICICICT); 2017: IEEE. 10.1109/ICICICT1.2017.8342581
19. Shaheed MNB, Sozer Y, Chowdhury S, De Abreu-Garcia JA, editors. A novel decentralized adaptive droop control technique for DC microgrids based on integrated load condition processing. 2020 IEEE Energy Conversion Congress and Exposition (ECCE); 2020: IEEE. 10.1109/ECCE44975.2020.9235785
20. Khanabdal S, Banejad M, Blaabjerg F, Hosseinzadeh N. A novel control strategy of an islanded microgrid based on virtual flux droop control and direct flux fuzzy control. International Journal of Engineering, Transactions B: Applications,. 2021;34(5): 1274-83. 10.5829/IJE.2021.34.05B.21
21. Xia Y, Wei W, Yu M, Wang X, Peng Y. Power management for a hybrid AC/DC microgrid with multiple subgrids. IEEE Transactions on power electronics. 2017;33(4):3520-33. 10.1109/TPEL.2017.2705133
22. Dragicevic T, Vasquez JC, Guerrero JM, Skrlec D. Advanced LVDC electrical power architectures and microgrids: A step toward a new generation of power distribution networks. IEEE Electrification Magazine. 2014;2(1):54-65. 10.1109/MELE.2013.229703
23. Guerrero JM, Vasquez JC, Matas J, De Vicuña LG, Castilla M. Hierarchical control of droop-controlled AC and DC microgrids—A general approach toward standardization. IEEE Transactions on industrial electronics. 2010;58(1):158-72. 10.1109/TIE.2010.2066534
24. Nasirian V, Moayedi S, Davoudi A, Lewis FL. Distributed cooperative control of DC microgrids. IEEE Transactions on Power Electronics. 2014;30(4):2288-303. 10.1109/TPEL.2014.2324579
25. Anand S, Fernandes BG, Guerrero J. Distributed control to ensure proportional load sharing and improve voltage regulation in low-voltage DC microgrids. IEEE transactions on power electronics. 2012;28(4):1900-13. 10.1109/TPEL.2012.2215055
26. Shafiee Q, Dragicevic T, Andrade F, Vasquez JC, Guerrero JM, editors. Distributed consensus-based control of multiple DC-microgrids clusters. IECON 2014-40th Annual Conference of the IEEE Industrial Electronics Society; 2014: IEEE. 10.1109/IECON.2014.7048785
27. Meng L, Dragicevic T, Guerrero JM, Vasquez JC, editors. Dynamic consensus algorithm based distributed global efficiency optimization of a droop controlled DC microgrid. 2014 IEEE international energy conference (ENERGYCON); 2014: IEEE. 10.1109/ENERGYCON.2014.6850587
28. Guo F, Xu Q, Wen C, Wang L, Wang P. Distributed secondary control for power allocation and voltage restoration in islanded DC microgrids. IEEE Transactions on Sustainable Energy. 2018;9(4):1857-69. 10.1109/TSTE.2018.2816944
29. Dehaghani MN, Taher SA, Arani ZD, editors. Distributed Secondary Voltage and Current Control Scheme with Noise Nullification Ability for DC Microgrids. 2020 10th Smart Grid Conference (SGC); 2020: IEEE. 10.1109/SGC52076.2020.9335768
30. Biglarahmadi M, Ketabi A, Baghaee HR, Guerrero JM. Integrated nonlinear hierarchical control and management of hybrid AC/DC microgrids. IEEE Systems Journal. 2021;16(1):902-13. 10.1109/JSYST.2021.3050334
31. Nabian Dehaghani M, Taher SA, Dehghani Arani Z. An efficient power sharing approach in islanded hybrid AC/DC microgrid based on cooperative secondary control. International Transactions on Electrical Energy Systems. 2021;31(6):e12897. 10.1002/2050-7038.12897
32. Zuo S, Altun T, Lewis FL, Davoudi A. Distributed resilient secondary control of DC microgrids against unbounded attacks. IEEE Transactions on Smart Grid. 2020;11(5):3850-9. 10.1109/TSG.2020.2992118
33. Guo F, Wang L, Wen C, Zhang D, Xu Q. Distributed voltage restoration and current sharing control in islanded DC microgrid systems without continuous communication. IEEE Transactions on Industrial Electronics. 2019;67(4):3043-53. 10.1109/TIE.2019.2907507
34. Fan B, Peng J, Yang Q, Liu W. Distributed control of DC microgrids with improved ZIP load adaptability. IEEE Transactions on Systems, Man, and Cybernetics: Systems. 2021;52(7):4623-33. 10.1109/TSMC.2021.3101813
35. Xing L, Mishra Y, Guo F, Lin P, Yang Y, Ledwich G, et al. Distributed secondary control for current sharing and voltage restoration in DC microgrid. IEEE Transactions on Smart Grid. 2019;11(3):2487-97. 10.1109/TSG.2019.2956515
36. Keshavarz M, Doroudi A, Kazemi M, Mahdian Dehkordi N. A new consensus-based distributed adaptive control for islanded microgrids. International Journal of Engineering, Transactions A: Basics. 2021;34(7):1725-35. 10.5829/IJE.2021.34.07A.17

Persian Abstract

چکیده

در سال‌های اخیر، ریزشبکه‌های DC به سبب افزایش گسترده منابع انرژی پراکنده و بارهاDC ، به همراه پیشرفت در فناوری‌های الکترونیک قدرت، توجه قابل توجهی را به خود جلب کرده‌اند. به منظور به‌کارگیری مؤثر ریزشبکه‌ها، استفاده از یک استراتژی کنترلی مناسب که ولتاژ ریزشبکه را در سطح مطلوب حفظ کند و تقسیم توان برابر بین واحدهای تولید پراکنده را تضمین کند، بسیار مهم است. جهت دستیابی به این اهداف، یک ساختار کنترلی دو لایه در این مقاله پیشنهاد شده است. در لایه اولیه، یک طرح کنترل شیب–افتی اصلاحی معرفی شده است که افت ولتاژ کمتری را در مقایسه با استراتژی‌های شیب–افتی سنتی به دست می‌آورد. همچنین، یک کنترل‌کننده توزیع‌شده بهبود دهنده ولتاژ در لایه ثانویه پیشنهاد شده است که دارای یک قسمت کمکی جهت بهبود دقت تقسیم توان نیز می‌باشد. استراتژی‌های کنترل پیشنهادی قابلیت اجرای ساده‌ای دارند و به شبکه ارتباطی و مخابراتی کم حجمی نیاز دارند. برای ارزیابی کارایی روش کنترل پیشنهادی، مطالعات موردی متعددی مانند تغییرات بار و چالش‌های قطع و وصل شبکه ارتباطی و اثرات نویز انجام شده‌است. علاوه بر این، عملکرد روش پیشنهادی در برابر طرح کنترل افتی اولیه سنتی و روش‌های کنترل ثانویه توزیع‌شده مشارکتی مقایسه شده است. مطالعات شبیه‌سازی انجام‌شده در نرم‌افزار MATLAB/SIMULINK نشان می‌دهد که روش کنترل پیشنهادی بهتر از روش‌های دیگر عمل می‌کنند و اثربخشی آن را در حفظ تنظیم ولتاژ و اهداف اشتراک توان تأیید می‌کند.